Supporting Information

IrO_xcore-shell nanocatalysts for cost-and energy-efficient electrochemical water splitting

Hong NhanNong[a], *Lin Gan*[a], *Elena Willinger*[b],
Detre Teschner[*,b], *Peter Strasser*[*,a]

[a] Department of Chemistry, Chemical and Materials Engineering Division, The Electrochemical Energy, Catalysis and Materials Science Laboratory, Technical University Berlin, Straße des 17. Juni 124, 10623 Berlin, Germany.

[b] Fritz-Haber-Institut der Max-Planck-Gesellschaft, Department of Inorganic Chemistry, Faradayweg 4-6, D-14195 Berlin, Germany.

[*]corresponding authors

Synthesis of supported $IrNi_x$ bimetallic nanoparticles

In a typical synthesis of $IrNi_3$NPs, 0.45mmol of Ni (II) acetate tetrahydrate (98%, Alfa Aesar), 0.66 mmol of 1,2-tetradecanediol [90%, Sigma Aldrich], 0.45 ml oleylamine [70%, Sigma Aldrich] and 0.45 ml oleic acid [99%, Alfa Aesar] were added to 45 ml dibenzyl ether [99%, Alfa Aesar] in a three-neck flask. The mixture was then heated to 80 ˚C and maintained at this temperature for 30 minutes under nitrogen flow to remove trace water. The temperature was then increased to 240 ˚C, and then 0.15mmol of $Ir(ac)_3$ [Chempur, 48% wt. Ir] was added to the reaction flask. The reaction solution was held at 240 ˚C for 1 hour and then cooled down to room temperature. 10 ml dichloromethane [99.8%, Merck] and 60 ml absolute ethanol [Merck] were added to the reaction mixture. In order to get the other desired Ir:Ni molar ratios of 1:2 and 1:5 in final products, the initial Ni a 0nd Ir precursor ratios were changed accordingly.

The as-synthesized $IrNi_x$ NPs were then supported on high surface area carbon to be used as electrocatalysts. In brief, a certain amount of Vulcan carbon black was ultrasonically dispersed in 30 mL of toluene. After that, the as-prepared $IrNi_x$ NP solution was added into Vulcan carbon black in the toluene and stirred overnight. The supported catalyst was washed with absolute ethanol several times and collected by centrifuge at 7700 rpm for 10 minutes. The slurry then was freeze dried for 20 hours. To remove the surfactants, supported $IrNi_x$ NPs were heated at 180 ˚C in synthetic air (25% Vol. of O_2 and 75% Vol. of N_2) for 2 hours. Then N_2 was purged into the furnace for 1 hour at 180 ˚C to remove O_2, after which the catalyst powders were further annealed at 400 ˚C in H_2 (4 vol% in Ar) for 4 hours. The Ir content in the supported catalysts was controlled to be ~ 20 wt% by adjusting the theoretical weight ratio of NPs to carbon support, but the real Ir weight loadings in the as-prepared materials were then evaluated by ICP-OES measurements.

Synthesis of supported pure Ir nanoparticles

In particular, 0.2 mmol of $Ir(CH_3COO)_3$ was dissolved in 40 mL of a 0.15 M solution of sodium hydroxide in ethylene glycol. The solution was degassed with nitrogen for 5 min and then heated under nitrogen flow, stirring and reflux to 160 ˚C and kept at this temperature for 30 min. Afterwards the reaction mixture was cooled down rapidly. 192.2 mg of Vulcan were suspended in 30 ml of ultrapure water and 5 ml of concentrated CH_3COOH by sonication for 10 min, and then Ir nanoparticle solution was added to the mixture, followed by stirring for 24 hours. The suspension was then centrifuged (10 min, 7700 rpm) and washed several times with ultrapure water. The collected Ir-Ni/support slurry then is freeze dried for 20 hours. The received powder is heat treated at 250 ˚C in N_2 atmosphere to remove remained organic substances.

Microscopic and spectroscopy characterization

*XRD.*XRD profiles were measured in Bragg−Brentano geometry in a D8 Advance X-ray diffractometer (Bruker AXS) using a Cu Kα source, variable divergence slit, and a position sensitive device as detector. Data were collected in a 2θ range of 20° to 95° with an increment of 0.05°, a measuring time of 5 s per step, and a sample rotation rate of 15 rotations per minute.

*ICP.*ICP-OES compositional analysis was performed using a 715-ES-inductively coupled plasma (ICP) analysis system (Varian). The standard concentrations were 1, 2, 4 and 6 ppm for Ir and Ni. The chosen wavelengths for concentration determination were 212.681, 224.268, 236.804, 254.397, and 263.971 nm for Ir and 216.555, 221.648, 222.295, 227.021, 230.299, and 231.604 nm for Ni.

*TEM.*TEM micrographs were acquired using a FEI TECNAI G^2 20 S-TWIN equipped with LaB6 cathode and GATAN MS794 P CCD camera. The microscope was operated at an acceleration voltage of 200 kV. The catalyst powders were suspended in ethanol; then the suspension was pipetted onto a carbon coated copper grid (400 mesh, Plano). Particle size distributions were determined by measuring around 200 particles using the ImageJ 1.46 software (U.S. National Institutes of Health).

*STEM-EDX.*High-resolution scanning transmission electron microscopy (STEM) and energy dispersive X-ray spectroscopy (EDX) line analysis were performed in FEI TITAN 80-300 electron microscope (300 kV) equipped with an image corrector (CEOS) and a high-angle annular dark field (HAADF) detector. The point resolution is 0.14 nm in HAADF-STEM mode. EDX spectra were collected across individual NP with drift correction at an acquisition time of 1-2 min/spectrum.

XPS-XAS.$IrNi_x$ catalysts were characterized by X-ray photoelectron and X-ray absorption spectroscopy at the ISISS beamline of the synchrotron facility BESSY of the Helmholtz-Zentrum Berlin. A detailed description of the setup can be found elsewhere.[1] Samples were mounted onto a sapphire sample holder and introduced into the spectrometer. The soft X-ray absorption spectra (XAS) of the Ni $L_{2,3}$ edge were recorded in the total electron yield mode. Both XAS and XPS experiments were carried out at room temperature (RT) in ultra-high vacuum (UHV). To calculate elemental ratios, the peak areas of Ir 4f, Ni 2p and O 1s were corrected considering the photon flux and tabulated cross sections.[2] A depth dependent experiment was performed also to estimate the distribution of metallic and oxidized Ir as a function of information depth. To do so, the Ir 4f core level was recorded at various photon energies yielding electron kinetic energies as 210, 550 and 1200 eV.

Working electrode preparation

To prepare the working electrode, a certain amount of carbon supported Ir-Ni catalyst was suspended in 2.490 mL of ultrapure water (Millipore, 18 MΩ), 2.490 mL of isopropanol and 20 μL of 5 wt% Nafion solution with sonication for 15 min to form a uniform ink. Ten μL of the ink was pipetted onto pre-polished and cleaned GC electrode and dried at 60 ^{0}C for 10 min in air, resulting in a uniform catalyst thin film. The amount of catalysts was calculated in order to get the final film on GC electrode containing 10.2 μg$_{Ir}$.cm^{-2}. All potentials reported in this paper were normalized with respect to the reversible hydrogen electrode (RHE).

Electrochemical protocols for synthesizing core-shell IrNi$_x$ nanoparticles

Metallic dealloyed IrNi@Ircore-shell nanoparticles (D-IrNi$_x$). Electrochemical dealloying (Step 1 in Figure 1) was performed by potential cycling between 0.05 V and 0.8 V for 200 cycles at 500 mV.s^{-1}~~/s~~. During the potential cycling, Ni was gradually dissolved and the surface was enriched by Ir.

*Stepwise oxidized (SO-IrNi@IrO$_x$) core-shell nanoparticles.*D-IrNi$_x$metallic core-shell nanoparticles were selectively surface oxidized (Step 2 in Figure 1) by cycling between +0.05 V and +1.5 V for 50 cycles at 500 mV.s^{-1}~~/s~~ to form stepwise oxidized *IrNi@IrO$_x$*metal-oxide hybrid core-shell nanoparticles. Afterwards, the potential was cycled between+0.4 V and+1.4 V at 20 mV.s^{-1}~~/s~~ three times to determine the charge under the Ir$^{III/IV}$redox peak, which was taken as an estimate of the number of active Irsites.

Directly oxidized (DO-IrNi@IrO$_x$)core-shell nanoparticles.~~D-IrNi$_x$- metallic core-shell~~Precursor alloy nanoparticles (PA-IrNi$_x$) were dealloyed and oxidized by applying potential cycling from +0.05 V to +1.5 V for 50 cycles at 500 mV.s^{-1}~~/s~~ (Step 3 in Figure 1). Afterwards, the potential was cycled between +0.4 V and +1.4 V at 20 mV.s^{-1}~~/s~~ three times to determine the charge under the Ir$^{III/IV}$ redox peak, which was taken as an estimate of the number of active Irsites.

Table S1. Atomic composition of supported pure Ir and IrNi$_x$ materials and their XRD, TEM based crystallite and particle size analysis

Sample	Weight content of Ir measured by ICP-OES, wt. %	Crystallite size evaluated by Debye-Sherrer equation, XRD, nm	Particle size evaluated from TEM image, nm
Pure Ir	20.4	1.5± 0.5	2.1±0.4
IrNi$_{2.3}$	18.5	5.4 ± 0.4	3.5 ± 0.6
IrNi$_{3.3}$	15.3	2.9 ± 0.2	7.2±2.0
IrNi$_{5.7}$	15.4	4.5 ± 0.2	13.9±5.6

The number-averaged mean particle sizes are higher than the mean crystallite sizes, may be due to partially amorphous domains inside the alloy particles and/or limitations of the applicability of the simple Debye–Scherrer equation to nanoscale clusters. [3]

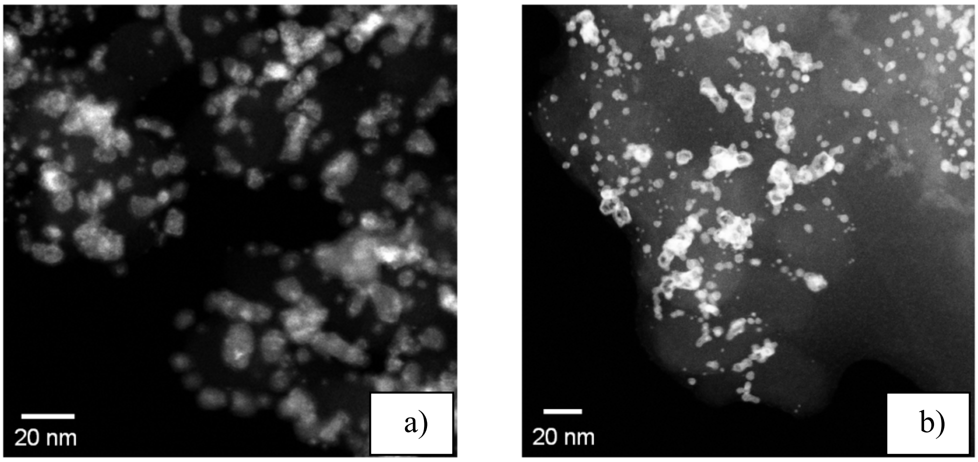

Figure S1.HAADF-STEM images of (a)PA-IrNi$_{3.3}$ and (b) D-IrNi$_{3.3}$ NPs

Iridium and Ni reveal a significant difference in the atomic number (Z = 77 for Ir and Z = 28 for Ni), which results in a distinct image contrast between Ir – and Ni rich specimen regions, similar to Pt and Ni.[4]The well alloyed PA-IrNi$_{3.3}$ catalyst shows a uniform contrast distribution with the highest intensity at the center of the particles, appearing as the brightest regions (Figure S1a).These contrast features indicate a homogeneous chemical composition. On the other hand, dealloyed NPs (Figure S1b) exhibit contrary HAADF patterns, in which NPs show bright rings (shells) surrounding dark inner parts (cores), indicating the formation of Ir enriched surface and Ni rich core nanostructures.

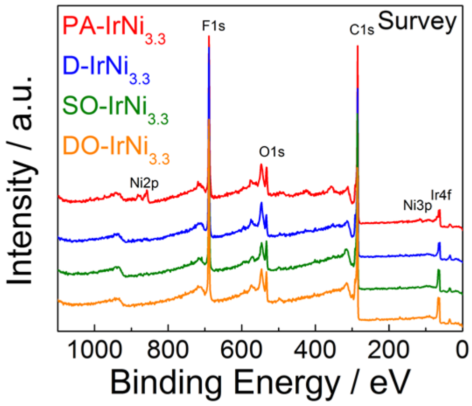

Figure S2. Survey XPS spectra of IrNi$_{3.3}$ series

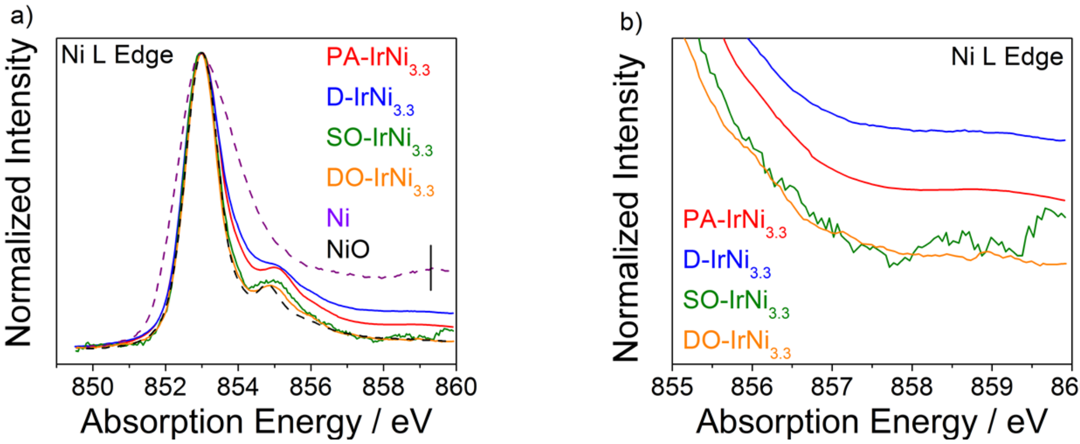

Figure S3.(a) Ni L-edge XANES of the IrNi$_{3.3}$ series and(b)a zoom on a tiny shoulder around 859 eV.

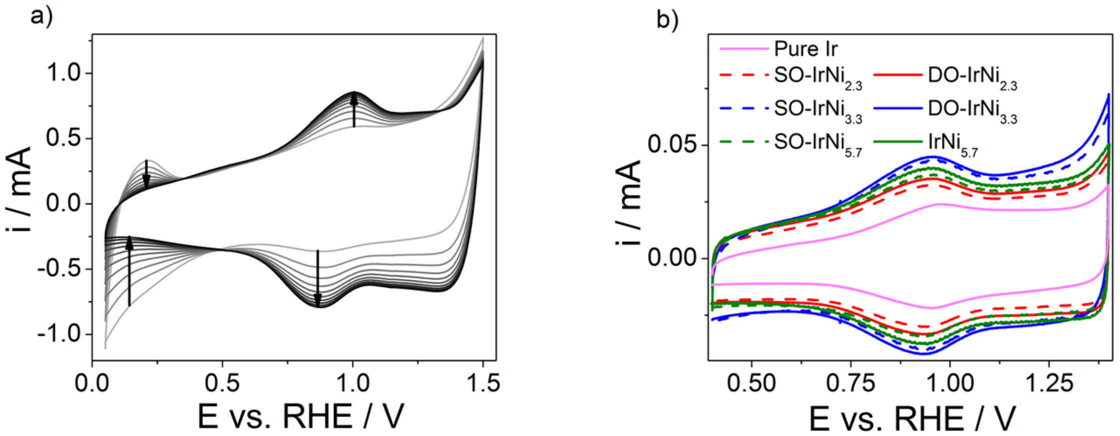

Figure S4.(a) Voltammetric surface oxidation PA-$IrNi_{3.3}$ catalystsand (b) Ir (III-IV) redox peaks of SO-$IrNi_x$ and DO-$IrNi_x$

Table S2. *Estimatedmolar amount of electrochemically accessible Ir redox sites of stepwise oxidized (SO-$IrNi_x$) and directly oxidized (DO-$IrNi_x$) samples*

	Pure Ir	$IrNi_{2.3}$	$IrNi_{3.3}$	$IrNi_{5.7}$
SO-$IrNi_x$ (nmol)	0.83	1.13	1.61	1.35
DO-$IrNi_x$ (nmol)	-	1.23	1.76	1.73

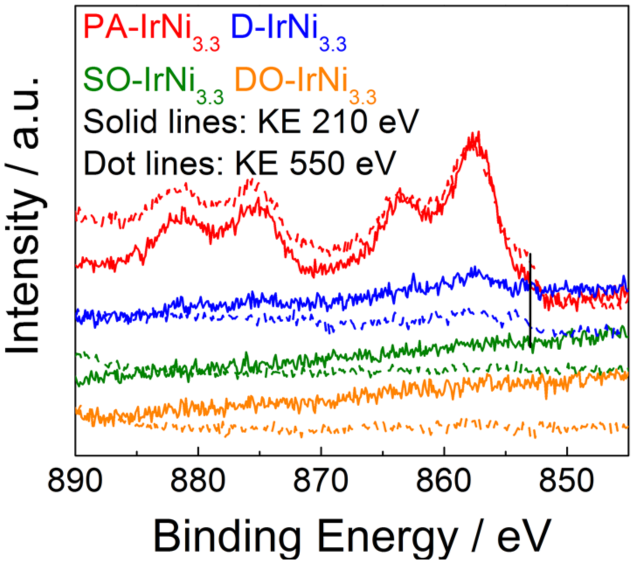

Figure S5. Ni2p of $IrNi_{3.3}$ series at two different photoelectron kinetic energies (KE).

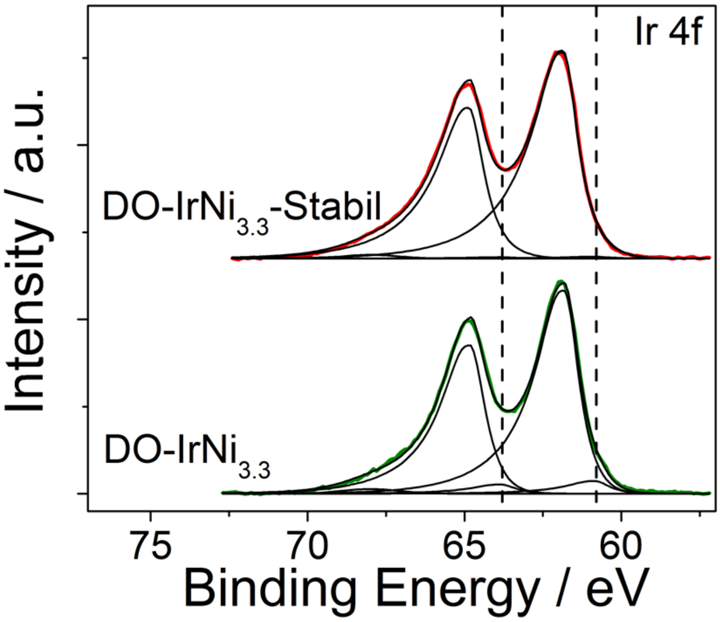

Figure S6. Ir4f XPS of directly oxidized IrNi$_{3.3}$ at photoelectron kinetic energyof 550 eV before stability test (bottom graph, denoted “DO-IrNi$_{3.3}$”) and after stability test (top graph, denoted “DO-IrNi$_{3.3}$-Stabil”) with Ir4f peak position derived from PA-IrNi$_{3.3}$ (dash lines) as standard for metallic Ir component.

References

(1) Knop-Gericke, A.; Kleimenov, E.; Hävecker, M.; Blume, R.; Teschner, D.; Zafeiratos, S.; Schlögl, R.; Bukhtiyarov, V. I.; Kaichev, V. V.; Prosvirin, I. P.; Nizovskii, A. I.; Bluhm, H.; Barinov, A.; Dudin, P.; Kiskinova, M. In *Advances in Catalysis*; Bruce, C. G., Helmut, K., Eds.; Academic Press: 2009; Vol. Volume 52, p 213.

(2) Yeh, J. J.; Lindau, I. *Atomic Data and Nuclear Data Tables***1985**, *32*, 1.

(3) Baranova, E. A.; Le Page, Y.; Ilin, D.; Bock, C.; MacDougall, B.; Mercier, P. H. J. *Journal of Alloys and Compounds***2009**, *471*, 387.

(4) Oezaslan, M.; Heggen, M.; Strasser, P. *Journal of the American Chemical Society***2012**, *134*, 514.